Electronic Supporting Information

A polymeric core-shell combinatorial nanomedicine for synergistic anticancer therapy

Asifkhan Shanavas[a], Nishant K. Jain[b], Navneet Kaur[a], Dinesh Thummuri[d@], Maruthi Prasanna[b], Rajendra Prasad [b], Vegi Ganga Modi Naidu[d], Dhirendra Bahadur[c#*] and Rohit Srivastava[b*]*

[a]*Institute of Nano Science and Technology, Habitat Centre, Phase-X, Sector-64, Mohali, Punjab 160062, India*

[b]*Department of Biosciences and Bioengineering, Indian Institute of Technology Bombay, Powai, Mumbai 400076, India.*

[c]*Department of Metallurgical Engineering & Materials Science, Indian Institute of Technology Bombay, Powai, Mumbai 400076, India.*

[d]*National Institute of Pharmaceutical Education and Research Guwahati, Nits Mirza Road Parlli Part, Guwahati Assam 781125.*

*Corresponding authors

@current address: University of Florida, Department of Pharmacodynamics, 1333 center drive basic sciences building, Gainesville, FL, USA 32610

#current address: Department of Mechanical Engineering, Indian Institute of Technology Goa, Goa College of Engineering Campus, Farmagudi, Ponda-403401, Goa

Characterization techniques:

The Carboxyl Methylation of Chitosan was confirmed using ^{1}H-NMR and FTIR analysis. The Nuclear Magnetic Resonance (Mercury Plus 300MHz (Varian, USA)) measurements of proton nuclei present in chitosan and carboxy methyl chitosan were

performed after dissolving the material in deuteriated trifluroacetic acid. Fourier Transform Infrared spectroscopy (Nicolet Instruments Corporation, USA) was performed by mixing the material with KBr followed by pelletizing and measuring the various covalent bond characteristics of modified and unmodified chitosan.

The fabricated nanoparticles were analyzed by transmission electron microscopes (TEM, CM200-Philips, 120 kV and HRTEM, JEM-2100F-Jeol, 200kV). Samples were analyzed after drop casting 10 µl on copper grids, stained with 1% (w/v) phosphotungstic acid solution and well dried under an infrared lamp. Scanning Electron Microscopy (SEM, JSM-7600F) analysis was carried out by casting diluted sample on ultraclean silicon wafer followed by gold sputter coating (10mA for 60 seconds) for making the polymeric sample conducting. Particle size distribution and polydispersity were measured using Dynamic Light Scattering (Brookhaven Instruments, USA). A 632 nm red laser was used in analyzing particles properly dispersed and diluted in double distilled water. Zeta potential (Zeta Potential Analyzer, Brookhaven Instrument Corp., NY, USA) of the samples was also measured. The quantification of dual drug formulations were carried out using High Performance Liquid Chromatography (HPLC) (waters alliance e2695) using acetonitrile and double distilled water in the ratio 80:20 as mobile phase.

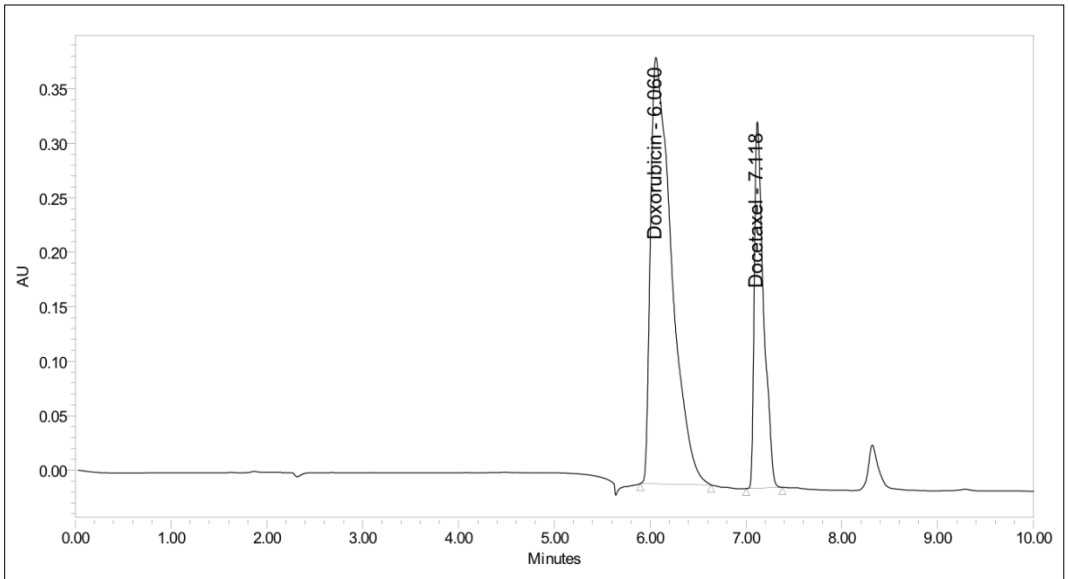

	Peak Name	RT	Area	% Area	Height
1	Doxorubicin	6.060	5917252	72.53	391342
2	Docetaxel	7.118	2241469	27.47	336207

Figure-S1. HPLC chromatogram of Dox and Dtxl extracted from dual drug nanoformulation

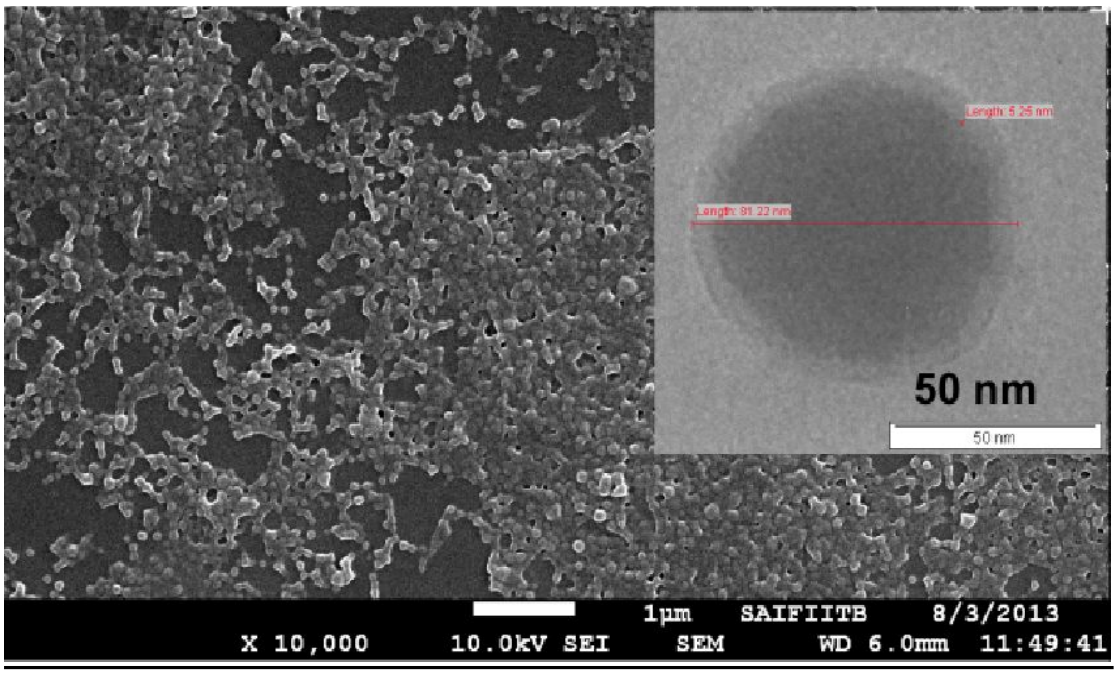

Figure-S2. SEM image of carboxy methyl chitosan coated blank cmcPLGA nanoparticles (A) and its corresponding TEM image.

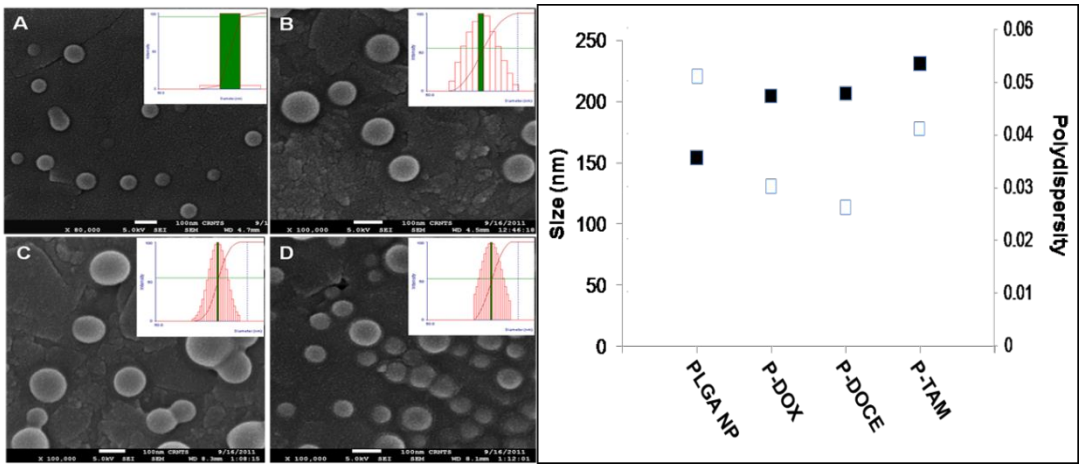

Figure-S3. SEM and DLS/PDI data showing blank (A) and drug (B-Docetaxel, C-Tamoxifen Citrate, D-Doxorubicin Hydrochloride) loaded PLGA nanoparticle size (actual and distributed). Filled squares – size; open squares – PDI

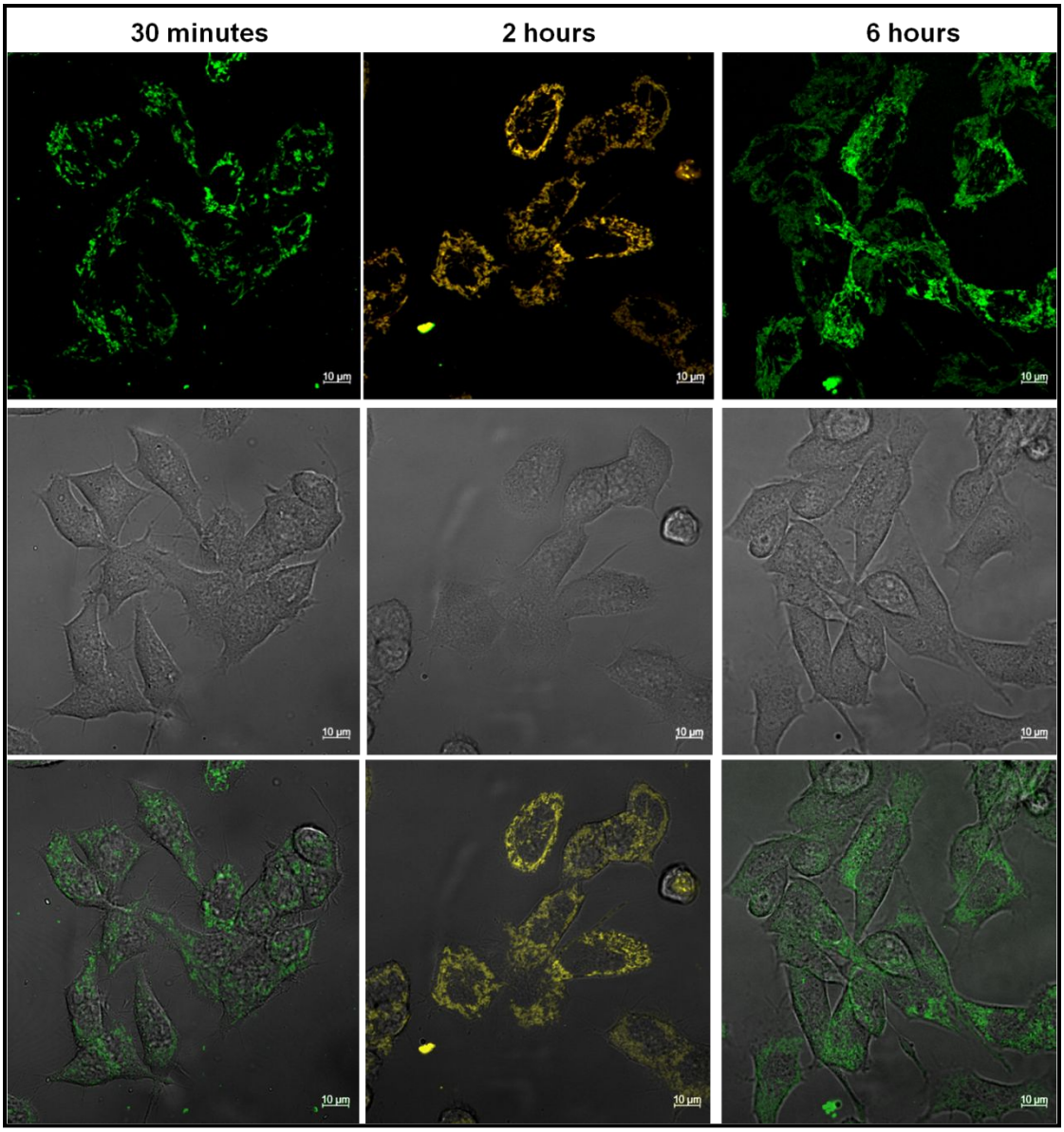

Figure-S4. Time dependant cellular uptake of cmcPLGA nanoparticles as visualized in form of fluorescence from Dox in the shell.

Table-S1. Comparison of IC50 values of Dox and Dtxl with previous literature

Cell line	Drug	IC 50 Value previously reported	IC 50 Value in the current manuscript	Reference
A549	Doxorubicin	0.61 μM	0.465 μM	1
	Docetaxel	4.26 nM	7.09 μM	2
BT 549	Doxorubicin	3.035 μM	3.3 μM	3
	Docetaxel	8.4 nM	1.14 μM	4
PC3	Doxorubicin	0.91 μM	3.3 μM	5
	Docetaxel	0.598 μM	0.26μM	6

References:

1. Chen, S.F.; Zhang, Z.Y.; Zhang, J.L. Meloxicam increases intracellular accumulation of doxorubicin via downregulation of multidrug resistance-associated protein 1 (MRP1) in A549 cells, *Genet Mol Res.* **2015**. https://doi.org/10.4238/2015.November.18.18

2. Yin, H.; Guo, R.; Xu Y.; Zheng, Y.; Hou, Z.; Dai, X.; Zhang, Z.; Zheng, D.; Xu, H. Synergistic antitumor efficiency of docetaxel and curcumin against lung cancer, *Acta Biochim Biophys Sin (Shanghai)*. **2012**. https://doi.org/10.1093/abbs/gmr106

3. Camirand, A.; Fadhil, I.;, Luco, A.; Ochietti, B.; Kremer, R. B. Enhancement of taxol, doxorubicin and zoledronate anti-proliferation action on triple-negative breast cancer cells by a PTHrP blocking monoclonal antibody, *Am J Cancer Res*. **2013.**

4. Risinger, A.L.; Dybdal-Hargreaves, N. F.; Mooberry, S. L. Breast Cancer Cell Lines Exhibit Differential Sensitivities to Microtubule-targeting Drugs Independent of Doubling Time. *Anticancer Res.* **2015**

5. Hameed, A.; Anwar, A.; Khan, K. M.; Malik, R.; Shahab, F.; Siddiq, S.; Basha, F. Z.; Choudhary, M. I.; Urease inhibition and anticancer activity of novel polyfunctional 5,6-dihydropyridine derivatives and their structure-activity relationship. *European Journal of Chemistry* **2013**. http://dx.doi.org/ 10.5155/eurjchem.4.1.49-52.701

6. Tsakalozou, E.; Eckman, A. M.; Bae, Y. Combination Effects of Docetaxel and Doxorubicin in Hormone-Refractory Prostate Cancer Cells, *Biochemistry Research International.* **2012**. http://dx.doi.org/10.1155/2012/832059